Hindawi
Geofluids
Volume 2022, Article ID 4178554, 12 pages
https://doi.org/10.1155/2022/4178554

Research Article

A Study on the Influence of Mining Depth on the Stress Distribution Characteristics of Stope Surrounding Rock

Shaobo Li,[1] **Lei Wang**,[1] **Qihan Ren**,[2] **Chuanqi Zhu**,[1] **Huaqiang Liu**,[1] **Huaiqian Liu**,[3] **and Lipeng Chen**[1]

[1]*State Key Laboratory of Mining Induced Response and Disaster Prevention and Control in Deep Coal Mines, Anhui University of Science and Technology, Huainan 232001, China*
[2]*CCTEG Chongqing Research Institute, Chongqing, China*
[3]*School of Energy and Mining Engineering, China University of Mining and Technology (Beijing), Beijing 100083, China*

Correspondence should be addressed to Lei Wang; leiwang723@126.com

Received 14 July 2022; Accepted 31 August 2022; Published 23 September 2022

Academic Editor: Liang Xin

The occurrence of severe mine pressure in stope is of high risk, and the mining depth is the main control factor which affecting the occurrence of mine pressure in stope. In order to study the influence law of mining depth on stope strata behavior, taking 11318E fully mechanized working face in Xieqiao Coal Mine of Huainan Mining Group as the engineering background, the stress distribution and evolution characteristics of stope surrounding rock under mining depth were studied by similar material simulation. And the evolution laws of mechanical characteristics of stope surrounding rock under different mining depths of 600 m and 1200 m were simulated. It is concluded that with the increase of mining depth, the damage range of surrounding rock on the mining field increases significantly. The initial collapse of the immediate roof above the working face is not affected by the mining depth. The periodic weighting caving step decreases with the increase of mining depth, and the height of two zones above the working face increases with the increase of mining depth. The stress transfer and evolution characteristics of the strata above the stope were revealed. The increase of front caving angle indicates that the pressure on the support of the working face is greater, indicating that the support of the working face should be strengthened with the increase of mining depth. The research results have a guiding role in the control of surrounding rock and disaster prevention of deep mine stope.

1. Introduction

According to the present situation of coal resources exploitation in China, the coal reserves below 1000 m are 2.95 trillion tons, accounting for 53% of the total reserves, and the number of deep wells with mining depth of 1000 m is increasing. The mechanical behavior and failure characteristics of coal and rock mass in deep mining face are quite different from those in shallow coal seam [1].

Before mining in deep mine, the coal and rock mass are in deep three-dimensional stress equilibrium state. The original stress equilibrium is broken due to the mining and excavation of coal, which promotes the redistribution of stress field, displacement field and energy field of surrounding rock in stope and roadway. Structural parameters of stope are the main factors influencing the distribution and evolution of stress field, displacement field, and energy field of surrounding rock [2–4]. The change of stope structure parameters directly affects the mining pressure and its appearance, which is related to the support load of working face and the control of surrounding rock [5–7]. As one of the main structural parameters of stope, mining depth directly affects the magnitude of mine pressure. With the increase of mining depth, the probability of coal wall spalling and floor heave increases, and the pressure of deep mine appears violently [8–11].

Domestic and foreign scholars have studied the influence of mining depth on the mechanical properties of coal and rock mass in stope. He et al. [12] summarized and analyzed the main differences between deep mining and rock

engineering mechanics characteristics of shallow mining and raised that with the increase of mining depth, the failure mechanism of rock was transformed from the brittle mechanical response in the shallow part to the mechanical response of deep extension behavior. Xie et al. [13–17] concluded that the basic mechanical properties of coal and rock mass at different depths are completely different and proposed that mining depth is a mechanical state determined by the level of ground stress, mining stress state, and surrounding rock properties and obtained that the post-peak characteristics of rock at different depths show different characteristics with the increase of depth. Kang [18] comparatively analyzed the ground stress state and the ratio of horizontal stress to vertical stress in shallow and deep coal mines and believed that the ground stress in coal mines increased with the increase of buried depth, and the horizontal tectonic stress in the ground stress field of deep coal mines showed a weakening trend and the vertical stress increased. Gao et al. [19] carried out the simulation test of in situ mechanics and failure characteristics of deep coal and rock and obtained the law that the strength of rock mass increases nonlinearly with the occurrence depth, and the strength of shallow rock mass is less affected by the loading rate.

Xie et al. [20–22] studied stress transfer and evolution of the surrounding rock of stope. It was found that there is a force chain system composed of a large number of force chains in the surrounding rock of the stope. A force chain arch composed of strong chain bundles is formed in the direction of the working face and the inclination direction, and a macroscopic stress shell composed of strong chain bundles similar to the ellipsoid shape is formed in the whole stope. The stress shell is the main bearing capacity system of the overlying strata. Wang et al. [23, 24] found that the formation load formed a complex weak-strong chain network in coal and rock mass based on photoelastic test principle. The force chain is not only the main form of load transfer in discontinuous and granular media but also the bridge connecting macroscopic mechanical behavior and microscopic interaction mechanism of granular media. Qi et al. [25, 26] obtained the vertical and horizontal stress distribution laws of intrusive rocks at different positions in the mining process and deeply analyzed the stress field characteristics of surrounding rock in shallow coal seam working face. Jiang et al. [27] established the mechanical model of abutment pressure in the stage of insufficient mining and full mining, obtained the distribution law of abutment pressure under different mining degrees, and put forward the concept of dynamic and static abutment pressure.

Some scholars also studied the influence of mining depth on mine pressure and its appearance. Xie et al. [28] concluded that with the increase of mining depth, the convergence of roadway sides and the convergence of roof and floor gradually increased. The growth trend of roadway deformation increases sharply when the buried depth reaches 1400 m~1500 m. Song et al. [29] believed that the mining depth was one of the main factors affecting coal wall spalling and concluded that with the increase of mining depth, the stress concentration coefficient of fully mechanized working face increased, but the failure range of coal wall remained basically unchanged. Du et al. [30] concluded that with the increase of mining depth, the advance abutment pressure in front of the coal wall increased, and the displacement of roof and floor and the step distance of periodic weighting decreased.

The above literature has qualitatively studied the relationship between the mechanical properties of coal and rock mass in stope and the mining depth and has not systematically studied the variation law of stress distribution and evolution characteristics of surrounding rock in stope with the mining depth. In this paper, the mechanical properties and stress distribution characteristics of stope surrounding rock affected by mining depth are studied by using a similar material simulation test method. The research results have theoretical significance for control of stope surrounding rock, working face and roadway support. This study will have an important impact on the safe and efficient mining and sustainable development of deep coal mines.

2. Experimental Scheme

2.1. Engineering Geological Background. The similar simulation test is based on 11318E comprehensive mining face of Xieqiao Coal Mine in Huainan Mining Group as the main engineering background, which is located in the east wing of the east two B mining area in three stages of No. 8 coal seam. The retrieval elevation of working face is from -511 m to -620 m, the ground elevation is +20.9 m ~ +27.5 m, the working face inclination length is about 190 m, the average coal thickness is 3.2 m, and the coal seam inclination angle is 13° on average.

The structure of No. 8 coal seam of 11318E comprehensive mining working face is simple and stable, the direct top of which is gray sandy mudstone, the average thickness is 3.8 m, and its basic top is light gray siltstone with an average thickness of 4.2 m. The direct bottom of which is dark gray mudstone with a thickness of 2.9 m, the old bottom of which is grayish white siltstone with a thickness of 2.8 m. The rock column parameters of this coal seam are shown in Figure 1.

2.2. Similarity Ratio Selection. According to the coal seam, roof, and floor of 11318E comprehensive mining face in Xieqiao Coal Mine, This test uses a similar simulation experimental system; the rock stress in the similar model is achieved by monitoring the strain gauges laid in the rock formation through strain gauges. The rock deformation in the similar model is achieved by monitoring the displacement measurement points arranged on the surface of the model through the digital scatterometer and the meridian. The similar simulation experimental shelf size was chosen by $L \times W \times H = 4200\ \text{mm} \times 2000\ \text{mm} \times 250\ \text{mm}$, with a simulated strike length of 320 m, a tendency length of 480 m, a height of 400 m, and a dip angle of coal seam as 13°. Considering the actual need to study the thickness of the object above and below the coal seam, according to the similarity criterion, the similar simulation similarity is taken as follows:

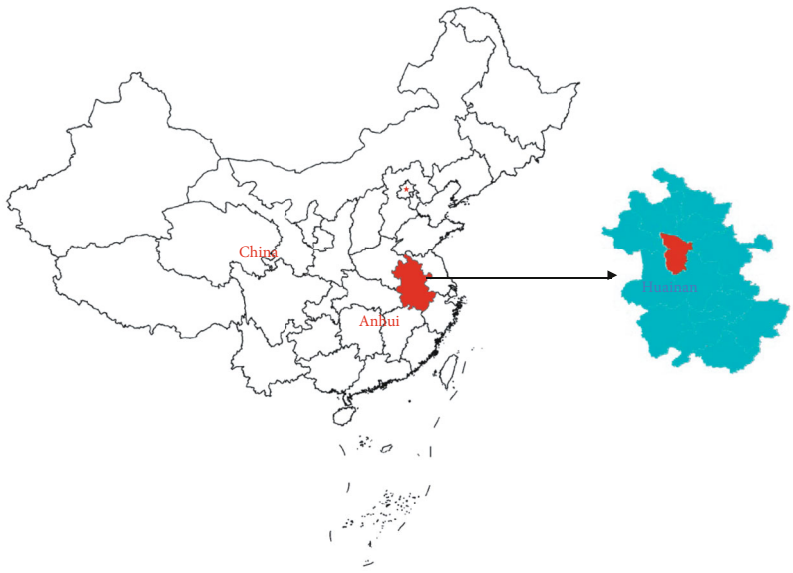

Columnar	Thickness/m	Lithology
	17.8	Quartz sandstone
	4.2	Siltstone
	4.0	Sandy mudstone
	3.2	8 Coal
	3.2	Mudstone
	3.0	Fine sandstone
	4.0	Mudstone
	3.2	Fine sandstone
	12.1	Medium sandstone
	5.0	Siltstone
	5.4	Mudstone
	2.6	6 Coal

Figure 1: Layout plan of fully mechanized 11318E coal mining face and roadway.

(1) Geometric similarity ratio is $C_L : C_L = 1 : 100$

(2) Bulk density similitude ratio is $C_\gamma : C_\gamma = 1 : 1.67$

(3) Stiffness similarity ratio is $C_E : C_E = 1 : 167$

(4) Strength similarity ratio is $C_\sigma : C_\sigma = 1 : 167$

2.3. Loading Pressure of Overlying Rock and Layout of Measuring Points. The similar materials selected for this similar simulation test include fine sand, gypsum, lime, and water to simulate the rock and coal seams, and the similar material proportioning scheme is determined according to the strength law of the coal body at different mining depths [11]. The joints between adjacent rock layers are simulated by scattering mica powder with uniform thickness.

Due to the limitation of the actual size of the similar simulation test bench, the rock layer could not be simulated from the excavation working face all the way to the surface. Therefore, the method of loading pressure is used to replace the weight of the overlying strata that cannot be simulated above the model.

In this paper, two similar simulation experiments were carried out to simulate the mining depth of 600 m and 1200 m, respectively. The simulated mining depth is 600 m, the simulation scheme similar ratio is set as 1/100, the model laying height is 1600 mm, the simulated roof rock height is 102 m, and the remaining 498 m height is realized by lever loading system above the model. According to the average capacitance of the overlying rock model is taken as 25 kN/m^3. Therefore, the stress magnitude generated at a depth of 498 m is 12.45 MPa.

$$\sigma = \gamma h, \tag{1}$$

where γ is the weight of overlying strata of coal seam, h is mining depth of coal seam, F_m is loading pressure of model, σ is stress, a_σ is strength similarity ratio, and S is the meaning of loading bearing area.

Based on the actual size and similar scale of the model, the actual loading pressure on the experimental system is 47.7 kN.

$$F_m = \frac{\sigma}{\alpha_\sigma} \times S. \tag{2}$$

When simulating the 1200 m mining depth, the simulation scheme is set as 1/100, the model laying height is 1600 mm, the simulated top rock height is 102 m, and the remaining 1098 m height is also realized by the loading system. According to the average capacitance of the overlying rock model is taken as 25 kN/m^3. Therefore, according to formula (1), the stress magnitude generated at the depth of 1098 m is 20.96 MPa. According to formula (2), the actual loading pressure for the 1200 m mining depth experimental system is 80.3 kN. Therefore, the loading pressure required to simulate the 600 m mining depth experimental system is 47.7 kN, and the loading pressure required to simulate the 1200 m mining depth experimental system is 80.3 kN.

In the similar model, the seam stress is measured by laying strain gauges in the bottom, direct roof, and main roof of the seam. The strain gauges record the deformation of the seam during the mining process through the sensor readings to calculate the stress. The rock deformation in the similar model is realized by monitoring the measurement points arranged on the surface of the model by digital scatterometer.

After the model is laid, displacement measuring points are arranged at an interval of 15 cm, and the measuring points in key monitoring areas such as open cut and stoping line are densified. A total of 281 displacement measuring points are arranged, as shown in Figure 2. Among them, the horizontal spacing of speckle measurement points in the red wireframe is 15 cm, and the horizontal spacing of speckle measurement points in the green wireframe is

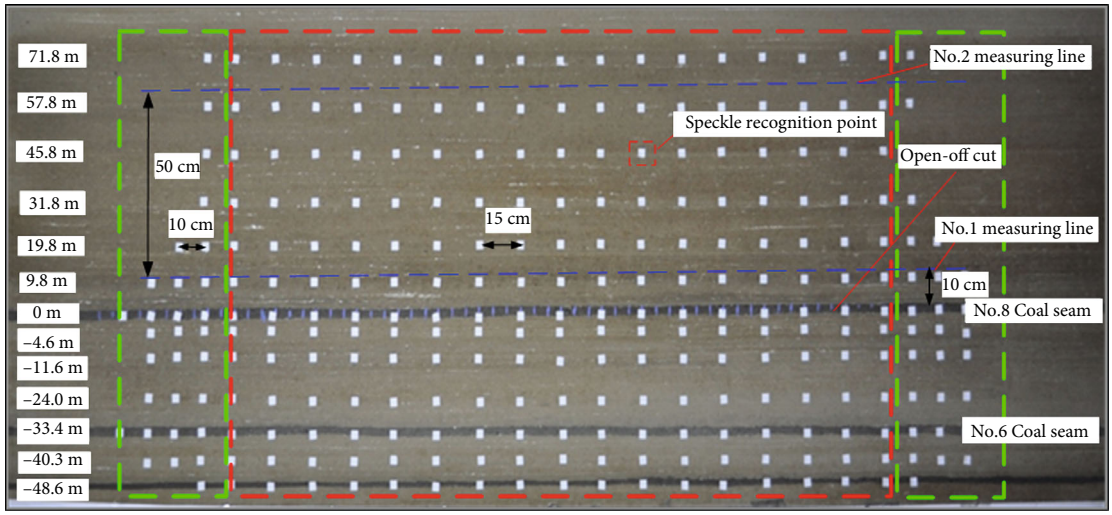

Figure 2: Layout of stress and displacement measuring points.

10 cm. The No. 1 and No. 2 survey lines are arranged for the stress survey line, of which the No. 1 survey line is 60 cm away from the floor of No. 8 coal seam and the No. 2 survey line is 10 cm away from No. 8 coal seam.

In this workface simulation mining process, since the 11318E working face actually advances 5 m per day, and 5 cm is advanced every 2 hours during the experiment. The specific mining process is as follows. Starting from the position of 80 m on the right side of the model, each mining length is 5 m and continues to mine after the overburden transport is stabilized, until it stops at the position of 240 m. During the experiment, the stress and displacement changes of the surrounding rock of 11318E working face were monitored and collected throughout the whole process, and the displacement, stress, and fracture of the surrounding rock during direct roof collapse and periodic incoming pressure were recorded, simulating the same mining process for both mining depths.

3. Influence of Mining Depth on the Evolutionary Characteristics of Stress Distribution of Surrounding Rock

3.1. Stress Field Distribution of Surrounding Rock in Stopes with Different Mining Depths. Two representative vertical measurement lines away from the opening cuttings by 80 m and 120 m are selected from the preburied stress sensors at the bottom and top of the coal seam. It can be found that the changes of stress at different burial depths of the overlying coal seam show obvious regularity in the process of working face advancement.

As shown in Figure 3, the stress change in the overlying rock layer when the 600 m mining depth working face is advanced to 120 m. It can be concluded that when the working face was advanced to 120 m, the collapse and sinking of the rock seam was intense, which led to the change of stress distribution 9.8 m, 33.7 m and 60.8 m from the floor of the coal seam, the overlying rock seam was more influenced by mining, and 80.6 m was less influenced by mining due to the far distance. The concentration of stress is most obvious around 15 m before and after the coal wall, and the concentration of stress decreases and returns to the original rock stress state 30 m away from the coal wall.

As shown in Figure 4, the stress variation of the overlying rock layer when the working face of 1200 m mining depth is advanced 120 m. It can be concluded that when the working face advances to 120 m, along with the collapse of the rock seam, the stress distribution state changes and is affected by mining at 9.8 m, 33.7 m, 60.8 m, and 80.6 m away from the floor of coal seam. The areas of stress-increased and stress-concentration appears in front of the open cut eyes and the coal wall. The stress concentration is most obvious around 23 m in front and behind the coal wall and gradually decreases and returns to the original rock stress state 35 m away from the coal wall.

Combining the above analysis of the stress change curves of each measuring point in the overlying rock layer during the advancing process of the working face at different mining depths, it can be concluded that when the working face advances to the same distance, the stress changes in the surrounding rock with different mining depths are different. With the increase of mining depth, the stress concentration area becomes larger, and the range influenced by high stress becomes wider. The rock layer affected by the mining area becomes larger, and the behavior of strata pressure becomes intense with the increase of mining depth.

3.2. Displacement Field Distribution of Mining Sites with Different Mining Depths

3.2.1. Results and Analysis of Similar Simulated Displacement Observations. For every 5 cm of excavation in the working face, the measuring points are photographed once by an industrial special camera, and the coordinate values of the measuring points are recorded by theodolite. In order to make the test results more accurate, every 20 cm excavation of the working face was taken as a node, and the

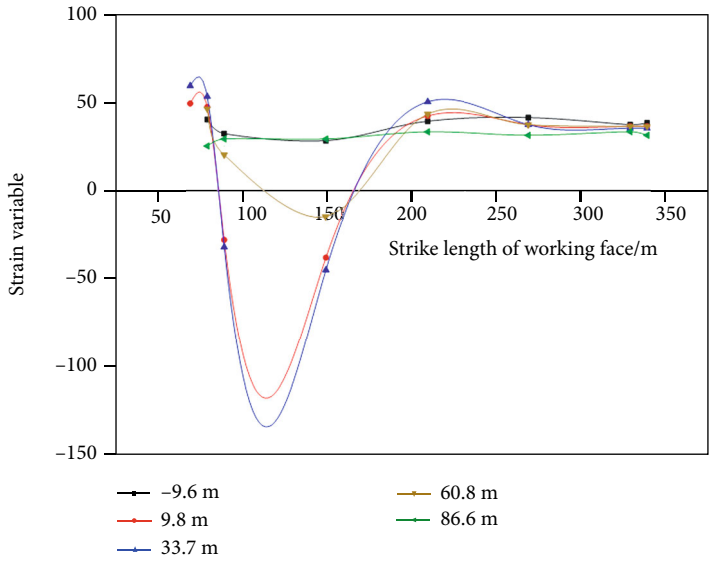

Figure 3: The stress variation curve of 600 m deep mining model when advancing 120 m.

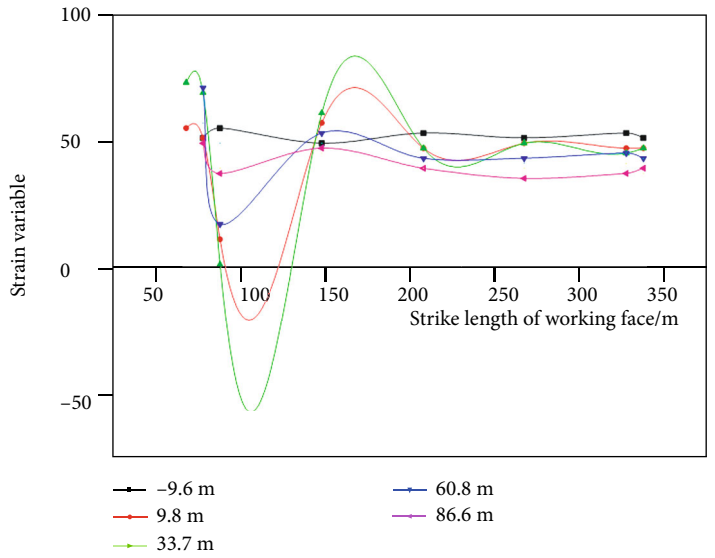

Figure 4: The stress variation curve of 1200 m deep mining model when advancing 120 m.

displacement analysis was carried out after the displacement deformation was stabilized, simulating the dynamic sinking changes of each measuring line caused by advancing the working face seven times. Mining depths of 600 m and 1200 m corresponded to the two measuring lines of No. 1 and No. 2, respectively.

The No.1 measurement line is 60 cm away from the vertical distance of coal seam floor, which is the least affected by mining, and the larger displacement change occurs only when the excavation reaches a certain distance. The No. 2 measurement line is 10 cm away from the coal seam, which is the most affected by mining, and the deformation displacement of the rock seam corresponding to this measurement line is the largest, and it can be seen from the figure that the change trend of the two measurement lines is approximately the same under the same mining depth.

The sinking curves of No. 1 line in the process of working face retrieval are shown in Figures 5 and 6.

In the No. 1 measuring line, which is far from the coal seam, the obvious displacement change appears only when the working face is excavated to 140 cm by the mining depth of 600 m, while the obvious displacement change appears when the working face is excavated to 120 cm with the mining depth of 1200 m. And the corresponding maximum vertical displacement increases from 15 cm to 24 cm with the increase of mining depth, and the horizontal scale corresponding to the maximum vertical displacement decreases from 75 m to 50 m.

It can be concluded from Figures 7 and 8 that with the mining of the working face, the sinking amount of the two measurement lines are increasing and reach the maximum at the middle of the mining area. The range of surrounding

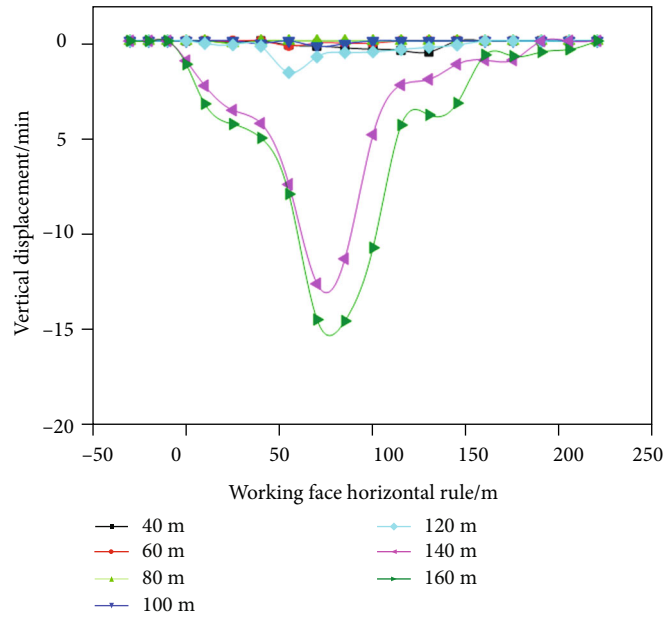

Figure 5: Dynamic subsidence curve of No. 1 line in the process of 600 m deep mining depth.

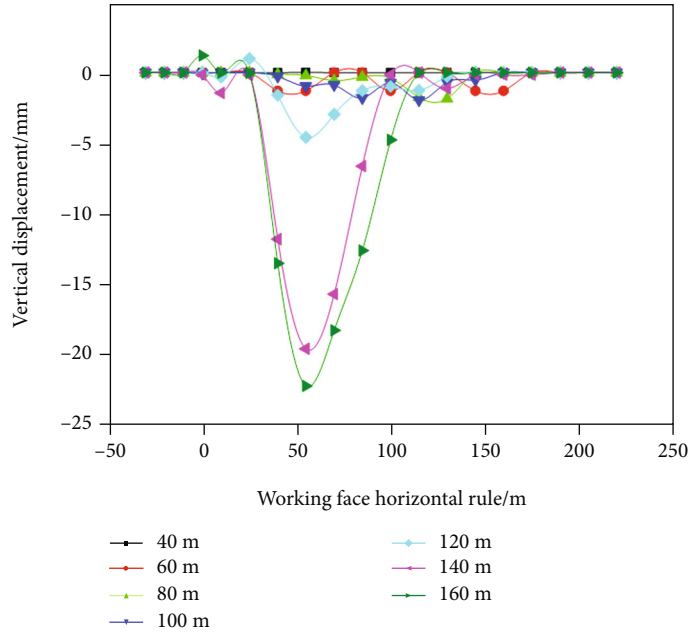

Figure 6: Dynamic subsidence curve of No. 1 line in the process of 1200 m deep mining depth.

rock movement deformation is expanding with the increase of mining depth, and with the advance of the working face, the movement deformation value in front of the coal wall gradually increases, while the movement deformation of the overlying rock layer in the back of the mining area becomes slower.

The sinking curves of No. 2 line in the process of working face retrieval are shown in Figures 7 and 8.

The displacement of No. 2 measuring line, which is nearest to the coal seam, increases continuously with the advancement of the working face at 600 m and reaches a maximum displacement of 25 mm when advancing to 160 cm, and the position corresponding to the maximum value is at 75 cm, while the maximum displacement at the advancement of the working face at 1200 m to 160 cm is 30 mm, and the position corresponding to the maximum value of displacement is at 45 cm, indicating that the position corresponding to the maximum value of displacement moves forward with the increase of the mining depth.

Comprehensive analysis shows that under the same mining depth; the balance of the original rock stress field is destroyed by the advancement of the working face, resulting in the redistribution of the three-dimensional stress field. The overlying rock layer in the mining area has different

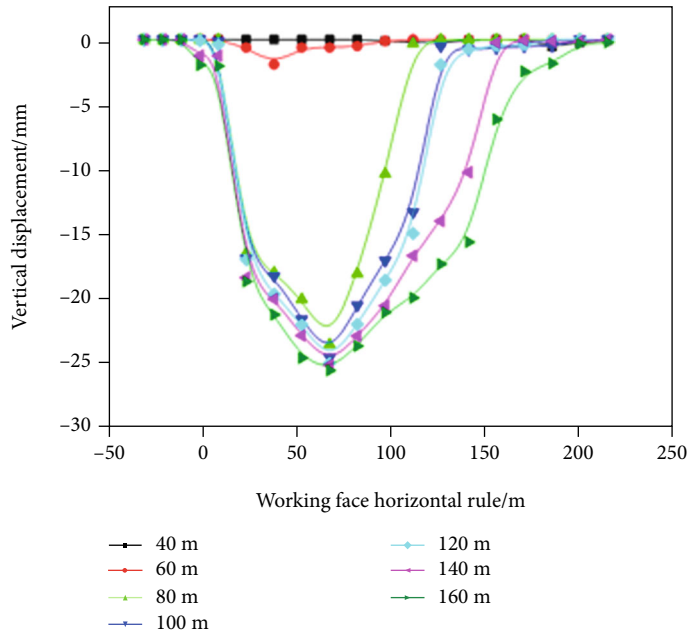

Figure 7: Dynamic subsidence curve of No. 2 line in the process of 600 m deep mining depth.

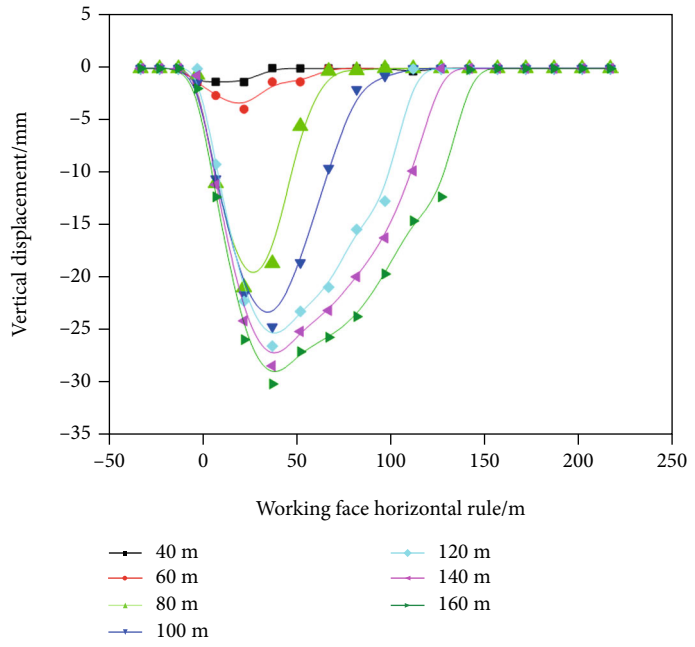

Figure 8: Dynamic subsidence curve of No. 2 line in the process of 1200 m deep mining depth.

degrees of subsidence and movement, forming a "U"-shaped deformation curve, and the maximum vertical displacement increases with the increase of the mining depth. The horizontal scale of the maximum displacement decreases with the increase of the mining depth.

3.3. Analysis of Displacement Cloud Map Changes. In order to observe more intuitively the settlement trend in the area composed of the two measurement lines, the difference between the above two measurement lines was fitted and the cloud plot to calculate the displacement values, as shown in Figures 9 and 10. It can be seen from the figure that with the excavation of the working face, deformation starts to occur when advancing 40 m, and the model produces obvious deformation when advancing 100 m, and the range of deformation influence zone becomes larger as the excavation proceeds. When the working face advances 160 m, the deformation zone is fully developed.

In the case of the same mining depth, the deformation of the overlying rock layer gradually develops upward during the working face advancement, the mobile deformation pattern of the surrounding rocks is similar, and the quarry area

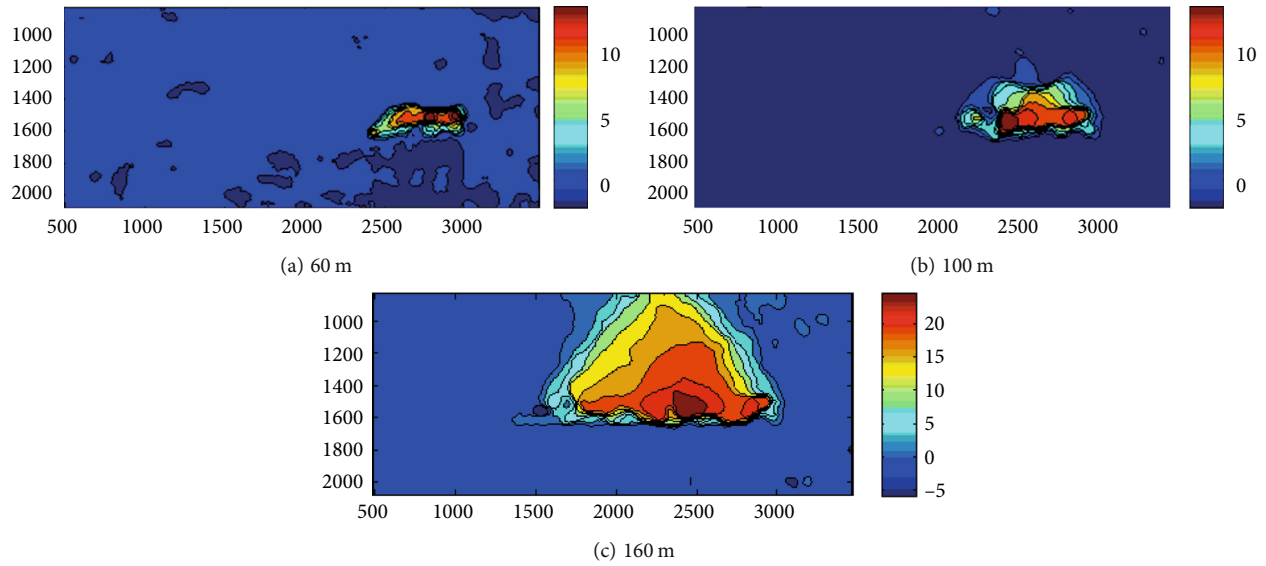

Figure 9: Nephogram of overlying strata displacement with excavation in a 600 m mining depth model.

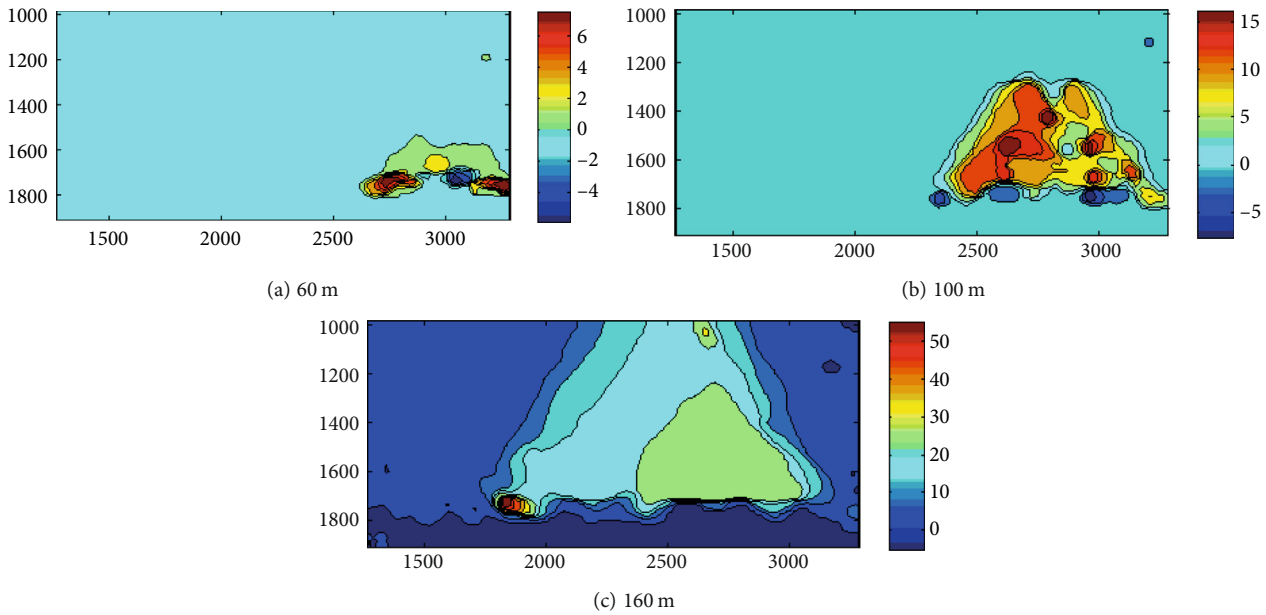

Figure 10: Nephogram of overlying strata displacement with excavation in a 1200 m mining depth model.

is filled with gangue across the fall. And the more distant from the coal seam floor the smaller the deformation of the surrounding rocks, the sinking curve of each rock layer presents an asymmetric pattern.

The absolute value of displacement gradually increases from No. 1 measuring line to No. 2 measuring line, indicating that the closer it is to the coal seam, the more obvious it is affected by excavation. The deformation of the surrounding rock is not obvious because No. 1 measuring line is far away from the coal seam, while No. 2 measuring line is the closest to the working face, the vertical displacement is the largest, and the deformation evolution pattern is the most obvious.

It can be seen from the comparison between Figures 9 and 10 that at the mining depth of 600 m, the absolute value of displacement gradually increases with the advancement of working face, and when the advancement distance reaches 160 m, the displacement value of overlying rock layer in the mining area reaches the maximum, and the maximum displacement value is 25 cm. With the advancement of working face, the absolute value of displacement also gradually increases at 1200 m mining depth, and when the advancement distance reaches 160 m, the maximum displacement value of overlying rock layer in the mining area reaches 50 cm.

Comparing the displacement evolution nephogram during the advancement of two mining depths, it can be seen that the greater the mining depth, the greater the vertical displacement of the overlying surrounding rocks on the working surface when the working surface is advanced to

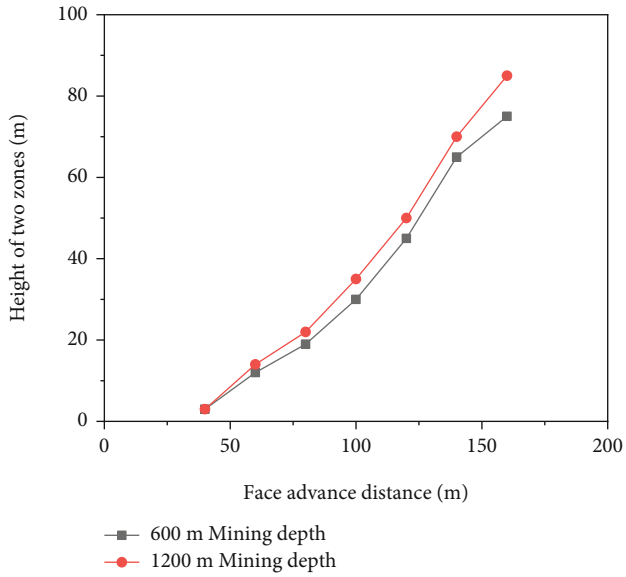

Figure 11: Change regulation of the height of two zones in different advancing distances of 600 m and 1200 m mining depth.

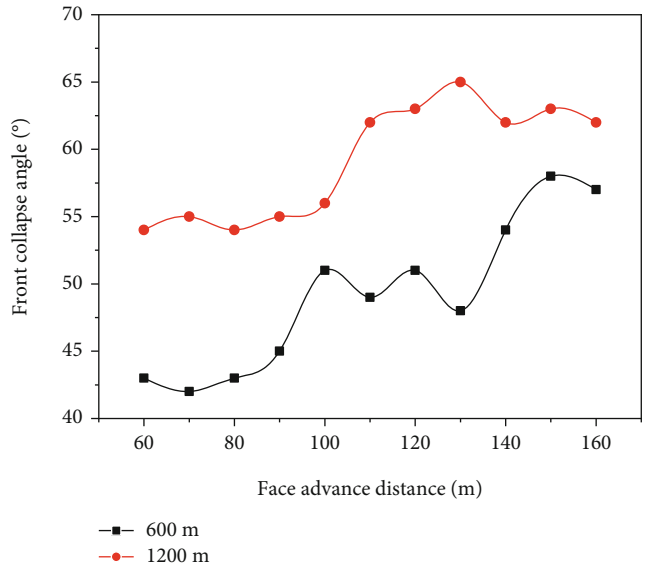

Figure 12: The change rule of the front caving angle with different advancing distance.

the same distance. And with the increase of the mining depth, the damage range of the surrounding rocks in the mining site has a more obvious increase.

4. The Effect of Mining Depth on the Damage Field of the Surrounding Rock

4.1. Mineral Pressure Manifestation in Quarries with Different Mining Depths. At 600 m mining depth, the phenomena in the mining process of similar simulated experiments were compiled and counted, and the phenomena in the mining process were described. When the working face is pushed to 40 m, the direct top collapsed for the first time with a collapse height of 3 m. When the working face is pushed to 50 m, the old top collapsed for the first time and the first cycle came to pressure; when it is pushed to 65 m, the second cycle came to pressure. When the working face is pushed to 80 m, the third cycle came to pressure and the fissure separation increased; when it is pushed to 95 m, the fourth cycle came to pressure and the height of the two zones was 30 m. When the working face is pushed to 110 m, the fifth cycle came to pressure and the height of the two zones was 45 m; when it is pushed to 160 m, the height of the two zones reached 73 m.

At 1200 m mining depth, the direct top collapsed for the first time at 40 m, with a collapse height of 3 m; the old top collapsed for the first time at 50 m with the first cycle to pressure, with the fourth cycle to pressure at 95 m, when the working face is pushed to 110 m, with the fifth cycle to pressure, and with a two-band height of 58 m. And when it is pushed to 110 m, the height of the two zones is 80 m.

At 600 m mining depth, with the back mining of the working face, the direct top rock of the coal seam then fell, the basic top and overlying rock layer collapsed periodically only after the direct top collapse, and when the working face advanced to 40 m, the direct top collapse gradually stabi-

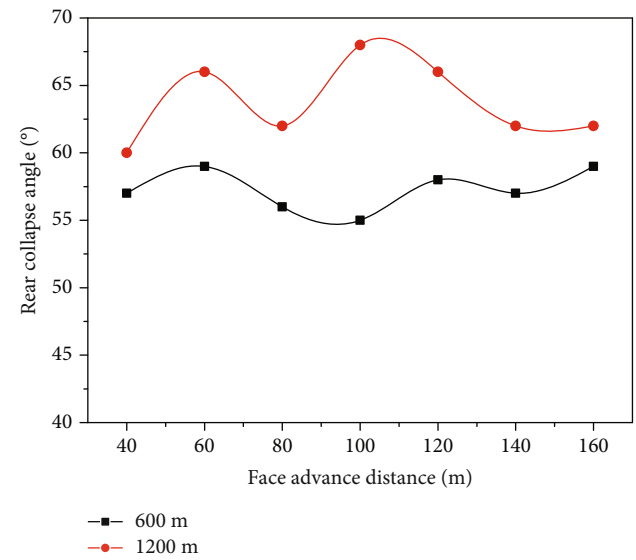

Figure 13: The change rule of the rear collapse angle with different advancing distance.

lized, the collapse height reached 3 m, and the direct top collapse step was 40 m. The overlying rock layer in the mining area moved and deformed during the back mining of the working face, when the working face pushed to 50 m, the upper part of the old top began to appear off-seam fissures, when the working face advanced to 55 m, the old top collapsed for the first time, the collapse height was 8 m, and after that the old top collapsed periodically, the average collapse step was 15 m. When pushing to 55 m, the old top collapsed for the first time, the collapse height is 8 m, after that the old top collapsed periodically, the average collapse step is 15 m, the incoming pressure periodicity is more obvious, and the collapse height of overlying rock and development

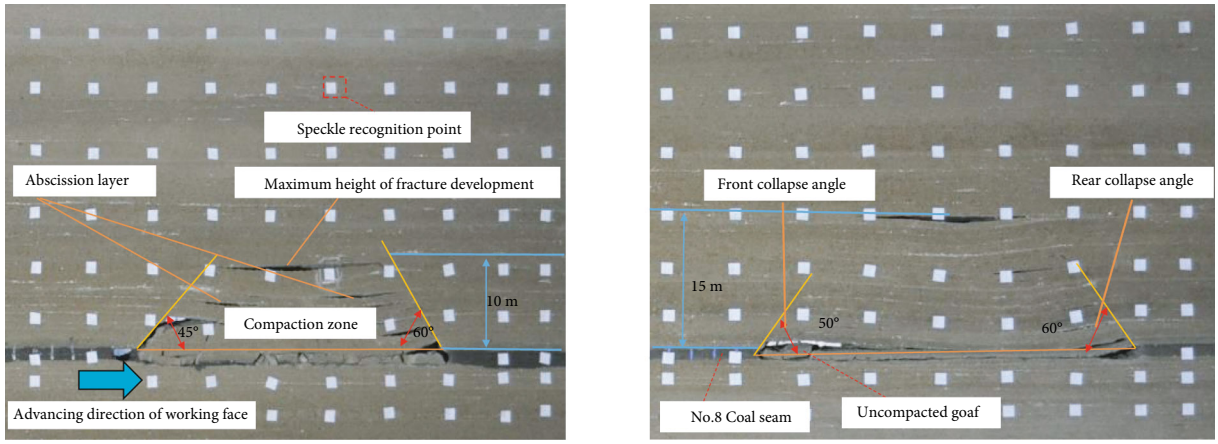

(a) Advance of 600 m and 1200 m deep mining face by 45 m

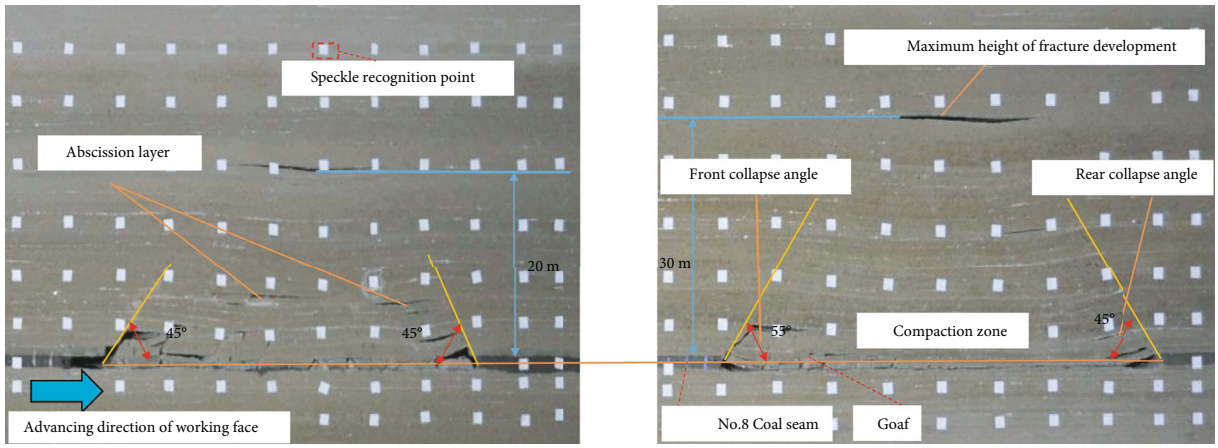

(b) Advance of 600 m and 1200 m deep mining face by 80 m

Figure 14: The deformation law of overlying strata under 600 m and 1200 m mining depth when advancing the same distance.

height of fissure also show increasing law with the advance of working face.

At 1200 m mining depth, the rocks within the direct top of the coal seam are mined along with the bubble, while the direct top and the overlying rocks start to collapse gradually when the working face is pushed to a certain distance, with the phenomenon of overhanging roof, when the working face is pushed to 40 m, the direct top collapse gradually stabilizes, the collapse height reaches 3 m, and the direct top collapse step is 40 m. When the working face is pushed to 45 m, the fissures above the old top start to appear, when it is pushed to 50 m, the old top collapses for the first time, the collapse height is 9 m, after that the old top collapses periodically, the collapse step is 10 m on average, the coming pressure periodicity is more obvious, and the overlying rock collapse height and fissure development height also show the increasing law with the advancement of the working face.

Along with the continued advance of the working face, the height of the two zones keeps developing upward. Figure 11 shows the variation law of two-zone heights at different advancing distances for different mining depths. Comparing with the variation law of two-zone heights at different advancing distances for 600 m mining depth, it is concluded that the rate of increase of two zone heights is greater in the case of 1200 m mining depth. The greater the mining depth, the greater the rate of increase in the height of the two zones.

4.2. Distribution of Damage Fields in Mining Sites with Different Mining Depths

4.2.1. Cross-Footing Characteristics. With the advancement of the working face, the upper uncollapsed rock layer appears delaminated, and then, the delaminated fissure continues to increase until it breaks, the deformation movement pattern of each rock layer overlying the mining area is basically similar, with the increase of the rock layer level, the main influence range and the maximum sinking amount of each rock layer gradually become smaller, and the pattern of the sinking curve is asymmetrical. Figures 12 and 13 show the variation law of collapse angle at different advancing distance of different mining depth. It can be seen from Figures 12 and 13 that with the continuous advancing of the working face, the rear collapse angle does not change much and the front collapse angle shows an increasing trend. And the front and rear collapse footings increase with the increase of mining depth.

Comparing the variation rule of collapse angle at different advancing distances under 600 m mining depth and

1200 m mining depth, it can be concluded that the front collapse angle increases when advancing to the same distance, and the rear collapse angle basically remains the same. The increase of front caving angle indicates that the pressure on the support of the working face is greater, indicating that the support of the working face should be strengthened with the increase of mining depth.

4.2.2. Deformation Damage Characteristics. Under different mining depths, the overlying rock collapse deformation characteristics of the model were photographed during the working face advance, and the overlying rock collapse movement deformation after mining the working face at different advance distances was obtained as shown in Figures 14(a) and 14(b).

It can be seen that from Figures 14(a) and 14(b), when the mining depth is 600 m and 1200 m, the direct top collapse step is 40 m, and the cycle pressure is more obvious, the cycle pressure collapse step for 600 m mining depth is 15 m, and the cycle pressure collapse step for 1200 m mining depth is 10 m; it can be seen that the increasing mining depth has no effect on the direct top initial collapse and the cycle pressure collapse step gradually decreases.

From the macroscopic fracture phenomenon of the surrounding rocks at different mining depths, it can be concluded that when the working face is advanced to 85 m, the height of the two zones at 600 m mining depth is 20 m, and the height of the two zones at 1200 m mining depth is 30 m, which shows that the height of the two zones increases with the increase of the mining depth, and with the continuous advance of the working face, the height of the two zones changes obviously.

5. Conclusions

By taking 11318E fully mechanized working face in Xieqiao Coal Mine of Huainan Mining Group as the engineering background, the stress distribution and evolution characteristics of stope surrounding rock under mining depth were studied by similar material simulation. The main conclusions are as follows:

(1) With the increase of mining depth, the stress concentration area becomes larger, the influence range of high stress becomes wider, the rock layer affected by the mining area becomes larger, and the behavior of strata pressure becomes intense with the increase of mining depth

(2) The balance of the original rock stress field is destroyed with the advance of the working face. The overlying rock layer in the mining area has different degrees of subsidence and movement, and the maximum vertical displacement increases with the increase of the mining depth; the position of maximum displacement is closer to the coal wall

(3) With the increase of the mining depth, the vertical displacement of surrounding rock on the working face increases. The damage range of the surrounding rock of the stope has increased obviously

(4) The initial collapse of the immediate roof above the working face is not affected by the increase of the mining depth. The periodic weighting caving step decreases with the increase of mining depth, and the height of the two zones above the working face increases with the increase of mining depth

(5) The increase of front caving angle indicates that the pressure on the support of the working face is greater, indicating that the support of the working face should be strengthened with the increase of mining depth

Data Availability

The data used to support the findings of this study are included within the article.

Conflicts of Interest

The authors declare that they have no conflicts of interest.

Acknowledgments

This study was supported by the Foundation of University-Level General Projects of Anhui University of Science and Technology (Grant No. xjyb2020-01), the Major Special Project of Science and Technology in Anhui Province (Grant No. 202203a07020010), the Collaborative Innovation Funding Project of Colleges and Universities in Anhui Province (Grant No. GXXT-2020-055), and the National Natural Science Foundation of China (No. 52004007).

References

[1] H. P. Xie, M. Z. Gao, R. Zhang, G. Y. Peng, W. Y. Wang, and A. Q. Li, "Study on the mechanical properties and mechanical response of coal mining at 1000 m or deeper," *Rock Mechanics and Rock Engineering*, vol. 52, no. 5, pp. 1475–1490, 2019.

[2] X. Liang, P. Hou, and Y. Xue, "A fractal perspective on fracture initiation and propagation of reservoir rocks under water and nitrogen fracturing," *Fractals*, vol. 29, no. 7, 2021.

[3] Y. Xue, J. Liu, X. Liang, S. Wang, and Z. Ma, "Ecological risk assessment of soil and water loss by thermal enhanced methane recovery: numerical study using two-phase flow simulation," *Journal of Cleaner Production*, vol. 334, p. 130183, 2022.

[4] Y. Xue, J. Liu, P. G. Ranjith, F. Gao, Z. Zhang, and S. Wang, "Experimental investigation of mechanical properties, impact tendency, and brittleness characteristics of coal mass under different gas adsorption pressures," *Geomechanics and Geophysics for Geo-Energy and Geo-Resources*, vol. 8, no. 5, p. 131, 2022.

[5] Y. Luo, "Influence of water on mechanical behavior of surrounding rock in hard-rock tunnels: an experimental simulation," *Engineering Geology*, vol. 277, article 105816, 2020.

[6] Y. Luo, F. Q. Gong, X. B. Li, and S. Wang, "Experimental simulation investigation of influence of depth on spalling characteristics in circular hard rock tunnel," *Journal of Central South University*, vol. 27, no. 3, pp. 891–910, 2020.

[7] C. Q. Zhu, S. B. Li, and L. Wang, "The investigation of strata control for ultrasoft coal seam mining," *Geofluids*, vol. 2022, Article ID 8130555, 15 pages, 2022.

[8] H. P. Xie, S. P. Peng, and M. H. He, *Basic Theory and Engineering Practice of Deep Mining*, Beijing Science Press, 2006.

[9] S. B. Li, L. Wang, C. Q. Zhu, and Q. Ren, "Research on mechanism and control technology of rib spalling in soft coal seam of deep coal mine," *Advances in Materials Science and Engineering*, vol. 2021, Article ID 2833210, 9 pages, 2021.

[10] L. Yuan, "Research progress of deep mining response and disaster prevention and control," *Journal of China Coal Society*, vol. 46, no. 3, pp. 716–725, 2021.

[11] C. Q. Zhu, S. B. Li, and Y. Luo, "Progressive damage process and failure characteristics of coal under uniaxial compression with different loading rates," *Shock and Vibration*, vol. 2021, Article ID 3360738, 12 pages, 2021.

[12] M. C. He, P. Xie, and S. P. Peng, "Research on rock mechanics in deep mining," *Rock mechanics and engineering*, vol. 16, pp. 2803–2813, 2005.

[13] H. P. Xie, F. Gao, and Y. Ju, "Quantitative definition and analysis of deep mining," *Journal of China Coal Society*, vol. 40, no. 1, pp. 1–10, 2015.

[14] H. P. Xie, "Research progress of deep rock mechanics and mining theory," *Journal of China Coal Society*, vol. 44, no. 5, pp. 1283–1305, 2019.

[15] Z. Zhang, H. Xie, R. Zhang et al., "Deformation damage and energy evolution characteristics of coal at different depths," *Rock Mechanics and Rock Engineering*, vol. 52, no. 5, pp. 1491–1503, 2019.

[16] S. Li, M. Gao, X. Yang et al., "Numerical simulation of spatial distributions of mining-induced stress and fracture fields for three coal mining layouts," *Journal of Rock Mechanics and Geotechnical Engineering*, vol. 10, no. 5, pp. 907–913, 2018.

[17] H. P. Xie, M. Z. Gao, and C. X. Fu, "Study on mechanical behavior of brittle-ductile transformation of deep rock at different depths," *Journal of China Coal Society*, vol. 46, no. 3, pp. 701–715, 2021.

[18] H. P. Kang, "Deep coal mine stress distribution characteristics and roadway surrounding rock control technology," *Coal Science and Technology*, vol. 41, no. 9, pp. 12–17, 2013.

[19] M. Z. Gao, M. Y. Wang, and H. P. Xie, "Study on in - situ disturbed dynamic behavior of deep coal rock," *Journal of China Coal Society*, vol. 45, no. 8, pp. 2691–2703, 2020.

[20] G. X. Xie, "Mechanical characteristics of macroscopic stress shell of fully mechanized caving face and surrounding rock," *Journal of China Coal Society*, vol. 30, no. 3, pp. 309–313, 2005.

[21] G. X. Xie, Q. M. Liu, and W. H. Zha, "Patterns governing distribution of surrounding-rock stress and strata behaviors of fully-mechanized caving faces," *Journal of Coal Science & Engineering(China)*, vol. 1, pp. 5–8, 2004.

[22] G. X. Xie, "Mechanical characteristics of macroscopic stress shell of fully mechanized caving face and surrounding rock," *Journal of China Coal Society*, vol. 44, no. 10, pp. 2945–2952, 2019.

[23] J. A. Wang, C. Liang, and W. D. Pang, "Photoelastic experimental study on evolution of bidirectional flow dynamic chain under biaxial loading of particles," *Geotechnical Mechanics*, vol. 37, no. 11, pp. 3041–3047+3064, 2016.

[24] J. A. Wang, X. G. Han, and W. D. Pang, "Experimental study on force chain structure and evolution photoelasticity of top coal and rock in fully mechanized caving mining," *Journal of Eng-ineering Science*, vol. 39, no. 1, pp. 13–22, 2017.

[25] J. F. Pan, Q. X. Qi, and D. B. Mao, "3DEC simulation study on the movement and stress evolution characteristics of impact roof," *Journal of Rock Mechanics and Engineering.vol.26*, vol. 1, pp. 3546–3552, 2007.

[26] Y. F. Ren and Q. X. Qi, "Study on stress field characteristics of surrounding rock in longwall mining of shallow coal seam," *Journal of China Coal Society*, vol. 36, no. 10, pp. 1612–1618, 2011.

[27] J. H. Liu, F. X. Jiang, and S. T. Zhu, "Evolution law and application research of dynamic and static abutment pressure in longw-all mining field," *Journal of Rock Mechanics and Engineeri-ng*, vol. 34, no. 9, pp. 1815–1827, 2015.

[28] H. P. Xie, H. W. Zhou, and D. J. Xue, "Research and thinking on de-ep mining and limit mining depth of coal," *Journal of China Coal Society*, vol. 4, pp. 535–542, 2012.

[29] Z. Q. Song, S. K. Liang, and J. Q. Tang, "Research on influencing factors of coal wall spalling in fully mechanized working face," *Journal of Hunan University of Science and Technology (Natural Science Edition)*, vol. 1, pp. 1–4, 2011.

[30] J. P. Du, X. C. Zhang, and W. Y. Jia, "The strata behavior and control characteristics of deep mine stope," *Journal of China University of Mining and Technology*, vol. 1, pp. 82–84, 2000.